1962

Mechanics of the Voussoir arch as applied to block caving

Christopher Haycocks

MECHANICS OF THE VOUSSOIR ARCH AS APPLIED TO BLOCK CAVING

BY

CHRISTOPHER HAYCOCKS

A

THESIS

submitted to the faculty of the

SCHOOL OF MINES AND METALLURGY OF THE UNIVERSITY OF MISSOURI

in partial fulfillment of the work required for the

Degree of

MASTER OF SCIENCE IN MINING ENGINEERING

Rolla, Missouri

1962

APPROVED BY

Rodney D. Caudle (advisor) Ray E. Morgan

R.F. Davidson Lange B Clark

TABLE OF CONTENTS

ABSTRACT

The theories of ground failure in massive rock with special reference to the problem of the mechanics of block caving were studied and evaluated.

The mechanics of arch or dome formation underground were studied quantitatively using the Voussoir arch theory. The effect of shear stress on the arch stability was considered and found to affect the system only when the arch height increased beyond certain limits.

A theory of the mechanism of ground failure in an undercut block using the dome theory was advanced. Photoelastic model studies were used to support the conclusions reached.

ACKNOWLEDGEMENTS

The author wishes to express his appreciation to Mr. M. T. Worley, Rock Mechanics Instructor at the Missouri School of Mines and Metallurgy, for his support and aid in the formulation of this research during his semester as advisor to the author.

The writer is also greatly indebted to Mr. R. D. Caudle, Research Instructor, for his guidance and advice during the study, and for his criticism of the manuscript.

Thanks are also expressed to Professor Bruzewski, for his aid in preparing the photographic plates included.

LIST OF ILLUSTRATIONS

LIST OF FIGURES

CHAPTER I

INTRODUCTION

The use of block caving is finding increasing use as a mining method due to its simplicity, increase in safety for the miners as compared with many conventional mining methods, and the considerable lowering of the mining costs per ton of ore mined compared with previously used methods. Since its introduction in 1885 the caving system of mining has been developed only slightly, and little is known of the mechanics of the method, either with regard to the forces that induce caving or the stress distributions in the draw system.

The mechanics of caving as occurs in ground above mine openings that have collapsed and those parameters which influence it, are only guessed at in the rock mechanics literature, although great quantities of money, time and effort are often spent to limit the effects of caving and control its action. The efficiency of these efforts is generally poor and it has been conceded better to acknowledge the possiblity of subsidence and plan accordingly, than to try and control it. Control is at present limited almost entirely to stratified rocks which lend themselves to mathematical interpretation and analysis of the behavior of caving ground.

The purpose of this study is to examine the stresses that

cause caving in massive rock from both a theoretical standpoint using the theory of the Voussoir arch, and from an experimental standpoint, using photoelastic models. In accomplishing this objective, the relationships of some of the parameters concerning caving to the quantitative estimation of the stability of underground openings in massive fractured ground were investigated. Lastly a possible qualitative explanation is given of the manner in which an opening fails and the way in which the cave line advances with special reference to block caving where intradosal material does not affect the ground movement.

CHAPTER II

REVIEW OF THE LITERATURE

Mechanics of Caving

A review of the literature on the block caving method of mining reveals that writers have concentrated mainly on description and working details of mines where the system is employed, rather than on the mechanics of the mining system. Literature dealing with the mechanics of block caving is limited to the works of two authors, other information related to the subject must be extracted from the general mining and rock mechanics literature.

Block caving may be explained briefly by saying that it is a system of mining whereby a block of ore is undercut completely and then is caused to fail and break up under its own body forces. Failure starts on the underside of the block and gradually moves upward, the horizontal limits of the cave being controlled where necessary by stopes and drifts. Ore must be drawn continually to allow for the increase in volume of the broken material, or the caving action is prevented.

The origin of block caving is attributed to E. F. Brown[1], who first used the method successfully at the Pewabic mine on the Menominee range in Michigan in 1895, and who reported its success before the Lake Superior Mining Institute in 1898.

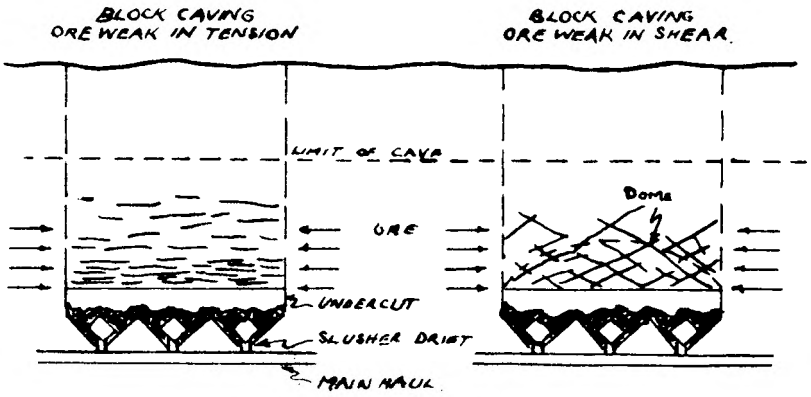

FIGURE (1)

Theory of block caving, after Bucky

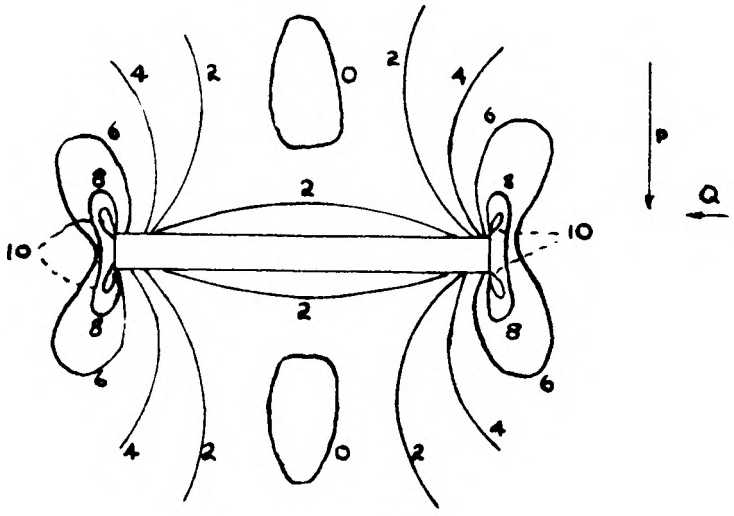

FIGURE (2)

Photoelastic stress distribution around a stope
after Isaacson

Since then the method has found wide application, and several variations on the original technique have been developed.

The first attempt to analyze the forces that produced caving was by P. B. Bucky[1]. He classified ore into two main types, (1) ore weak in tension, and (2) ore weak in compression. It was concluded that when the lateral stresses were in excess of the strength of the rock then the ore would fail and caving would occur; i.e., failure would occur in tension or compression according to the characteristics of the rock concerned. This analysis of the problem can be shown to be erroneous, the major criticisms being summarised as follows.

(1) The criteria for failure suggested by Bucky are independent of the width of the opening. This is not true in practice, as it has been found that the width of an opening is one of the major features affecting its stability, and that the wider it is, the more liable it is to failure.

(2) The use of boundary weakening drifts and stopes would serve to relieve the stresses that Bucky attributes caving to. In practice the stopes and drifts are found to weaken the block and aid its failure rather than prevent it.

(3) Photoelastic studies of the stress distributions around wide openings under stress fields with lateral constraint do not support Bucky's hypothesis. Stress concentrations do not occur as Bucky assumes, as can be seen in Figure 2, nor are they of the magnitude that Bucky predicted.

(Note the reference to a dome in the figure after Bucky, which was not explained in the text.)

This theory did however provide quantitative results and allowed calculation of volumes and types of rock suitable for caving.

Another more qualitative approach to the problem was suggested by J. B. Fletcher[3] in his description of the caving at the Miami mine, Arizona. He stated that the ore first failed in tension in the back, (top of the opening), until a dome was formed, and if the width of the opening was great enough, the dome was unstable and failed in compression. It was assumed that the rock composing the dome acted as an arch, which ultimately failed. This idea was also put forward by S. D. Woodruff[4].

The failure of ground around mine openings, or the formation of a "relieved zone" has been given much attention in rock mechanics literature although for large openings such as stopes, much of the work is purely speculative[3,4,5,6,7,8]. Most of this work has been based upon application of the theory of elasticity, which due to the assumptions made before its application, i.e., homogeneity, isotropy, etc., gives at the best, only a broad picture of what is happening in practice.

The dome theory in modified forms is used by most writers to explain the failure of ground around a mine opening.

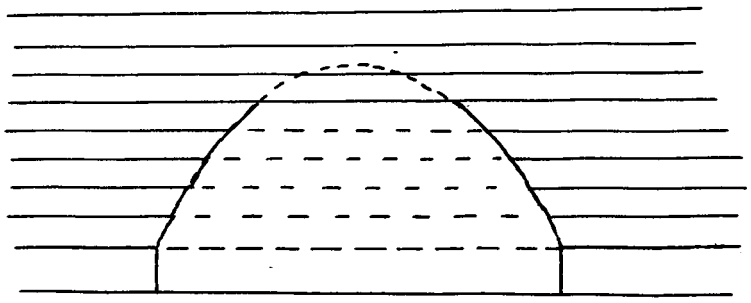

FIGURE (3)

Dome formed in stratified rock, after Fayol

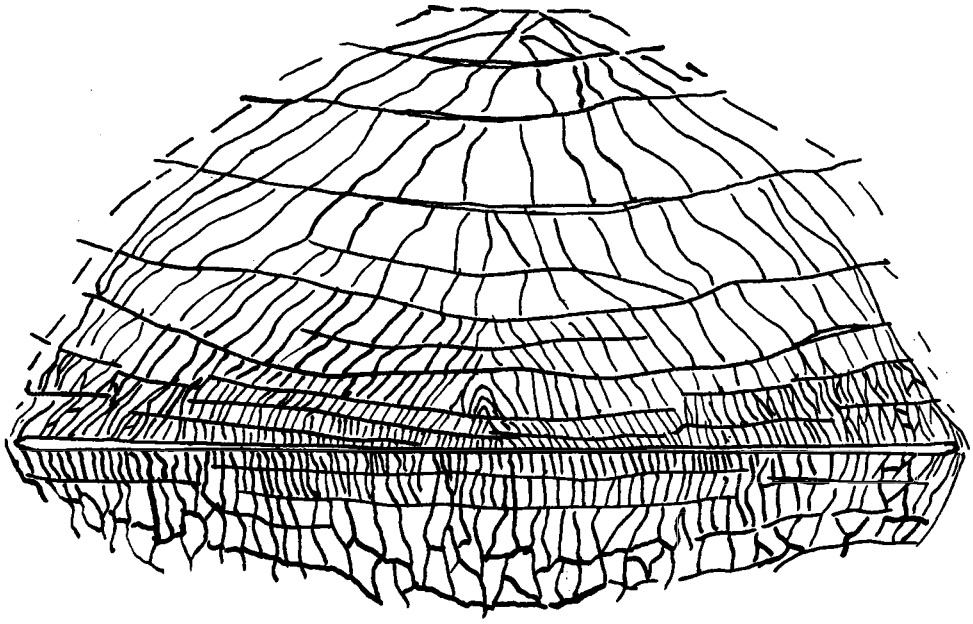

FIGURE (4)

Fracture zone around an excavation at depth, after Denkhaus

The general concept of the theory is that when an opening is made underground, the rock around the opening will often fail, and caving will continue until the opening has assumed a dome-shaped form, after which equilibrium is apparently established. Thus the stresses that accumulated originally around the edges of the excavation are now distributed evenly, and tend to "flow" around the excavation.

The dome theory was first put forward by Fayol[5] in 1885 after his famous model studies, which were confined to stratified rock. He postulated that the hanging wall consisted of a series of independent beams with fixed ends. Failure of these beams occured due to inward shearing at the end, giving rise to a dome shape, as in Figure 3 . Since that time, many attempts have been made to apply the dome theory to massive rock, although the exact mechanics of formation and final shape of the dome is still unknown.

The concept of a dome, as applied to massive rock, was first put forward by Kommerls, his work later being supported by R. Fenner[6], who theoretically derived its shape to be eliptical, using the theory of elasticity. H. G. Denkhaus[7] thought this to be an over simplification in the case of mine openings, and that in practice the eliptical form would be modified by the presence of the intradosal material, and the type of applied stress field, Figure 4 .

In 1946, C. J. Irving[8] postulated the existence of a

stress envelope around a mine opening, the ultimate shape of the envelope above the opening being semi-circular. His conclusions were however developed from information taken exclusively from the Witwatersrand gold mines in the Union of South Africa. F. Mohr[9] in 1946 also postulated an elliptically shaped dome where the ratios of the semi-axes of the elipse would vary with the ratios of the vertical and lateral free-field stresses. His relationship is:-

$$\frac{b}{\ell} = \frac{zz}{xx} = \frac{1-u}{u}$$

where:- b = height of the dome from the central axis.

ℓ = semi-width of the dome.

zz = vertical stress.

xx = Poisson's ratio.

As hydrostatic field conditions are reached, the ratio of the axes equals unity, and the dome shape approaches semi-circular, as was postulated by Irving.

J. R. Dinsdale[10] concluded, after making actual observations in a Cornish mine, that the dome shape in massive rock would be parabolic. In the work by W. H. Evans[11] (see appendix A) on the mechanics of the Voussoir arch as applied to massive strata, it was derived theoretically that the outline of a natural arch would be parabolic. His equation for the maximum allowable width of the arch is:-

$$L = \sqrt{\frac{8 f_m T}{w}\left(\frac{n}{2} - \frac{n^2}{6}\right)}$$

where:- f_m = compressive strength of the rock.

L = maximum allowable span of arch.

T = thickness of the beam containing the arch.

w = density of rock in pounds/cubic foot.

n = some fraction less than one; i.e., for optimum strength 0.5.

This derivation was made assuming that the rock was incapable of carrying tensile stresses due to its highly fractured nature, a common phenomena in rock suitable for block caving. The Voussoir or "natural" arch has been used since Roman times in the construction of buildings and bridges, and is normally constructed of a number of wedge-shaped pieces, arranged in an arch so that the load is thrown on the abutments. Such an arrangement may form naturally in heavily fractured ground when an excavation is made.

G. P. Manning[12] determined that the equation of the thrust line in a natural arch was parabolic under symmetrical and uniform loading. The profile, meaning the curve passed through the centroids of all the cross-sections, was represented by a continuous, smooth curve referred to rectangular coordinates, as shown in Figure 5 . The exact equation of this curve was not known, but it was assumed that it could be approximated by the linear polynomial,

$$y = a + bx + cx^2 + dx^3 + ex^4 + \ldots\ldots\ldots$$

As more terms are taken, the approximation above becomes more accurate. Now if four values of x are taken evenly spaced along the curve, say x_1, x_2, x_3, and x_4, and the corresponding

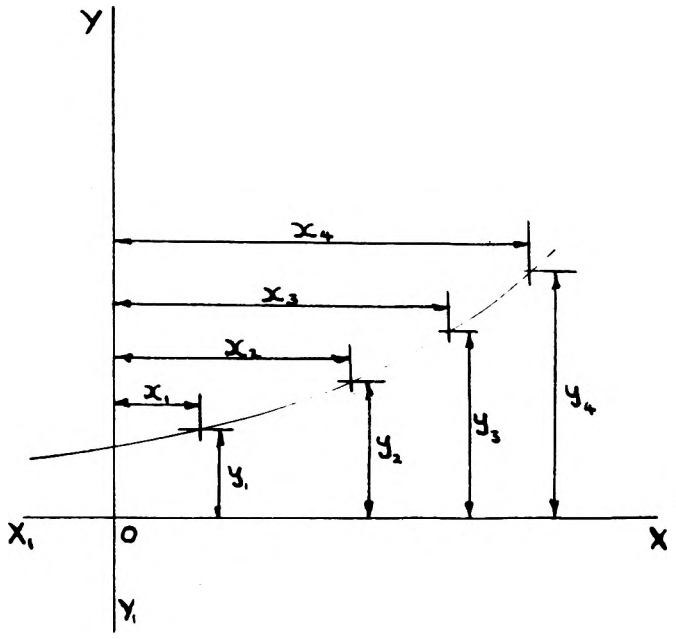

FIGURE (5)

Random curve representing arch profile, after Manning

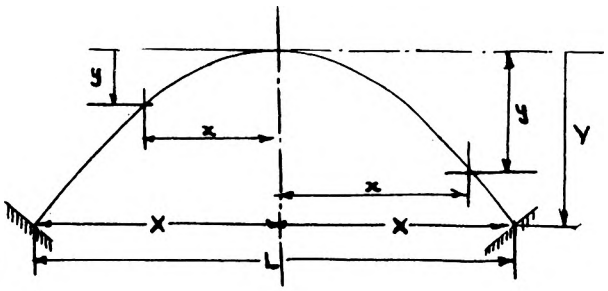

FIGURE (6)

Profile of symmetrical arch, after Manning

y values are y_1, y_2, y_3, and y_4, then:-

$$y_1 = a + bx_1 + cx_1^2 + dx_1^3$$
$$y_2 = a + bx_2 + cx_2^2 + dx_2^3$$
$$y_3 = a + bx_3 + cx_3^2 + dx_3^3$$
$$y_4 = a + bx_4 + cx_4^2 + dx_4^3$$

A solution to these simultaneous equations gives the values of the constants a,b,c,d. Figure 6 represents the profile of a symmetrical arch, after Manning, horizontal and vertical coordinates being measured from the crown for each half of the arch, where

$$y = a + bx + cx^2 + dx^3 + ex^4 + \ldots\ldots\ldots$$

and $$\frac{dy}{dx} = b + 2cx + 3dx^2 + \ldots\ldots\ldots\ldots\ldots$$

Since $x = 0$ when $y = 0$, then $a = 0$.

Also, since the arch is smooth and horizontal at the crown, $\frac{dy}{dx} = 0$ when $x = 0$, and therefore $b = 0$.

The first approximation of this curve is therefore:-

$y = cx^2$, which is a parabola.

The work by Bucky and Evans provides the only two theories that lend themselves to an actual quantitative analysis. The work by Fenner and Mohr gives only a broad indication of a possible dome size under ideal elastic conditions. As the work by Bucky has been largely discredited, the work by Evans is the only theory to date that can be used in practice to determine the criteria for stability of an opening in massive rock that has been fractured to some extent, as is almost invariably the case in practice. Evan's work is how-

ever limited to massive strata, and does not take complete account of the effect of shear stress across the abutments as the arch increases in height.

The calculation of the stresses around mine openings with different shapes, has been performed by many authors by application of the theory of elasticity. The results support Mohr's conceptions as to the shape of a stable opening underground, however, it is not unreasonable to assume that this shape would be modified in the case of actual mine rock which rarely if ever fulfills the requirements of the theory of elasticity. Although calculations based on the Voussoir theory, as by Evans, where no tensile strength is assumed, also represent an unrealistic condition, they may be very close appriximations for certain types of mine rock.

Model Study and Photoelastic Analysis

The use of models for the study of a mine structure is generally necessary due to the high cost, time and labor involved in producing a suitable prototype, and the difficulty in controlling the experimental conditions during a full scale test. For analysis of the stresses and their distribution around a mine opening, a photoelastic model is invaluable, since the time and cost in getting a similar stress picture around a prototype would be too great to be practical.

When models are to be used to study a structure it is

necessary not only to scale down the dimensions of the prototype but also the pressures, forces, displacements, stresses, etc.. The equations relating these factors are grouped together under the heading "Principles of Similitude". M. Hetenyi[13] gives a concise and complete account of the principles of similitude including the possible geometrical shape of the model in respect to the shape of the prototype. For general purposes, the model must be designed so that the behavior of the prototype may be deduced from the behavior of the model. Where models that are to be tested inside their elastic range are used, any elastic material may be used to simulate the prototype. To fulfill the requirements of the principles of similitude, when models simulate structures loaded by their own weight it is necessary that the effective unit weight of the model increase in inverse proportion to the model scale factor.

In the case of mine models it is best that the models be loaded by body force as is the case with the prototype. In practice it is usually not possible to increase the density of the model and at the same time reduce its rigidity to cause it to deform and therefore the remaining parameter, that of acceleration, is varied. This is done by testing the model in a centrifuge, thus the materials composing the model become apparently much denser, and a good replica of what happens in practice to the prototype is obtained.

Models fabricated from birefringent materials may be analyzed by photoelastic techniques, an account of which is given by Frocht[14]. The technique of photoelasticity may be said briefly to use the ability of certain plastics to selectivity retard light passing through them when they are under conditions of stress. This retardation, moreover, is directly proportional to the average maximum shear stress over the path of the ray. It follows that if a model is made of a suitable plastic and loaded, when it is viewed under polarized light a series of colored fringes will be apparent, and these fringes will represent contours of maximum shear stress existing within the model. It is then usually possible to determine the areas and points of greatest maximum shear stress and therefore, the places most liable to failure.

A modified stress freezing technique as suggested by J. W. Dally[15] is of considerable value in model studies. In this, a model is cast from clear epoxy resin and allowed to cure. Before the curing process is complete, the model is put under load and the curing process allowed to continue to completion. The strains induced in the model are retained upon removal of the load, and the model can be examined photoelastically at a later date, in the usual manner. By this means fringes may be "locked in" models which would be virtually impossible to study while under load.

CHAPTER III

THEORETICAL INVESTIGATION OF THE VOUSSOIR ARCH

Introduction

The following derivation of equations, involving criteria for the formation and stability of a Voussoir arch, as applied to massive rock, is a continuation of the work first put forward by Evans. (See appendix A). Evans's work was exclusively with thick beams and he did not take complete account of the shear forces induced across the vertical plane joining the beam to the abutment, which become appreciable as the arch height increases.

Theoretical Development

Evans explains that the Voussoir arch is normally a statically indeterminate structure, but under the conditions assumed, i.e., uniform loading, and solving for the maximum stress only, a very good approximation can be obtained by solution of the problem using simple statics.

It was assumed, by Evans, that the moment of resistance of any beam or arch to a load includes, (1) the moment of resistance developed as a simply supported beam, (2) the moment of resistance due to any horizontal thrust, i.e., for any section the product of the thrust and the vertical

distance between the line of thrust and the center of area of the section, and (3) the moment of resistance due to end fixing moments. Thus the total moment of resistance is the sum of the above moments. He states that, for stability, the maximum stress induced in the beam under a given set of conditions must not exceed the compressive strength of the material composing the arch.

Before commencing the analysis of the arch, the following assumptions must be made regarding the material composing the beam. The first five of these assumptions were taken directly from Evans's work. The sixth was proposed by the author.

(1) The rock behaves elastically under compressive stress.

(2) The material has no tensile strength by virtue of the many fractures that occur in it.

(3) Although the rock is highly fractured, sufficient shear strength for stability is generated by frictional resistance due to the compressional forces acting on the beam.

(4) The beam or arch is continuous with the adjacent country rock.

(5) Elastic strain of the abutments under horizontal compressive stress is negligible. This can be substantiated by calculation.

(6) Elastic strain of the abutments under a vertical compressive stress is negligible.

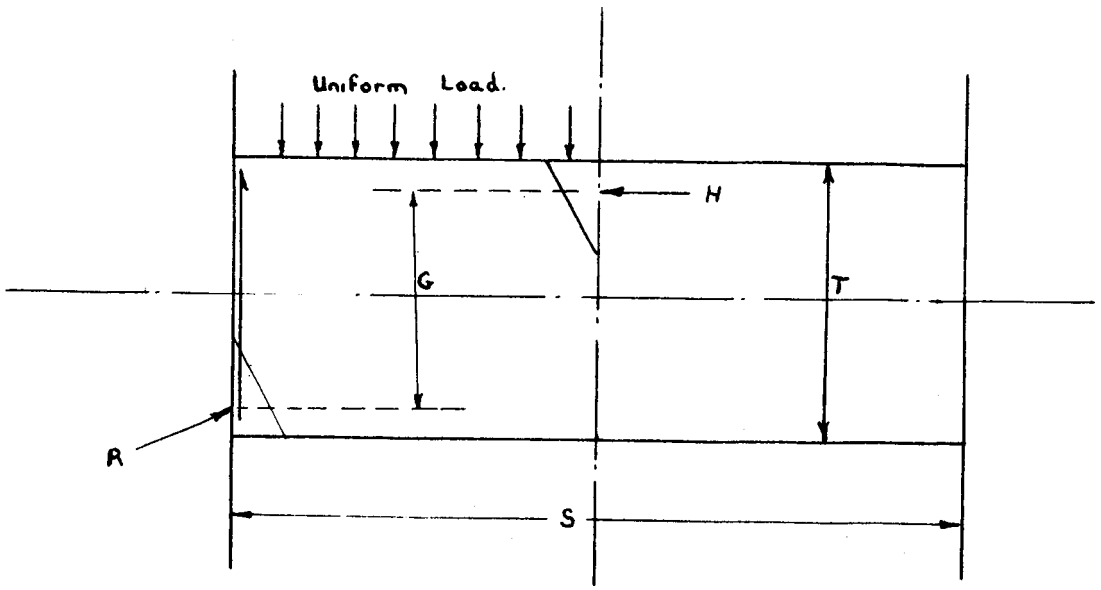

FIGURE (7)

Major force distribution in a Voussoir beam

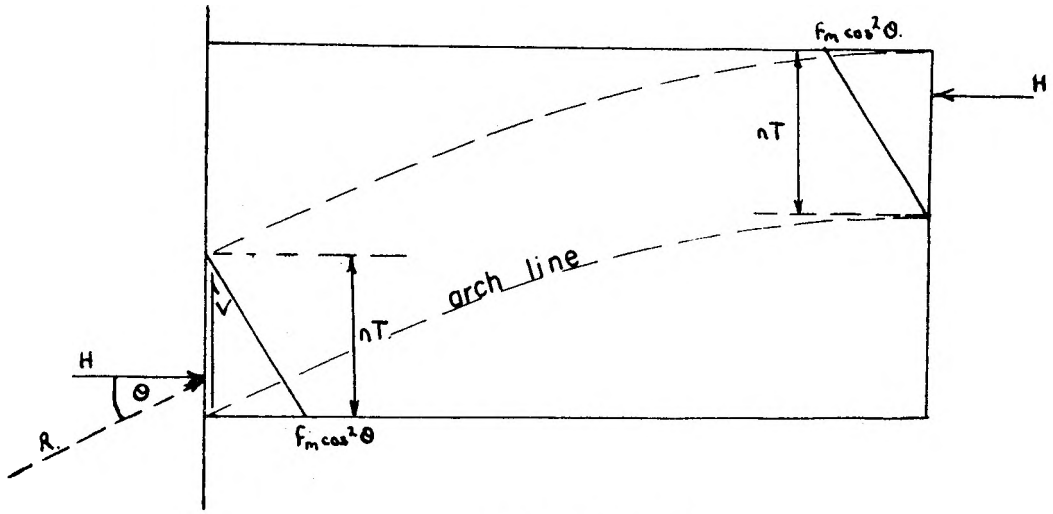

FIGURE (8)

Detailed force diagram for one half of a Voussoir beam

Before the moment of resistance can be calculated, it is first necessary to examine the stresses acting on the arch components and their resultant effect on the strength of the arch.

A general section of the arch, showing the major stresses and their distribution throughout the arch is given in Figure 7

In Figure 8 a more detailed view of one half of the arch is given. The major compressive stress R at the abutment has been divided into its component parts along the vertical and horizontal axes. The relationship between these forces taken from the Figure is:-

$$V = R \sin \theta \quad \text{.....(1)}$$

$$H = R \cos \theta \quad \text{.....(2)}$$

Therefore, $V = H \tan \theta$ .....(3)

Manning has shown that the outline of a natural arch is parabolic, with the general equation of the outline being:-

$$y = cx^2$$

For any arch profile, the value of c can be evaluated in terms of the width and height of the arch, as illustrated in Figure 9 . Thus:-

$$y = \frac{4\ G\ x^2}{L^2}$$

To find the tangent of the slope at the abutment the above expression is differentiated with respect to x.

$$\frac{dy}{dx} = \frac{8 \times G}{L^2} = \tan \theta$$

Therefore at the abutment where $x = \frac{L}{2}$

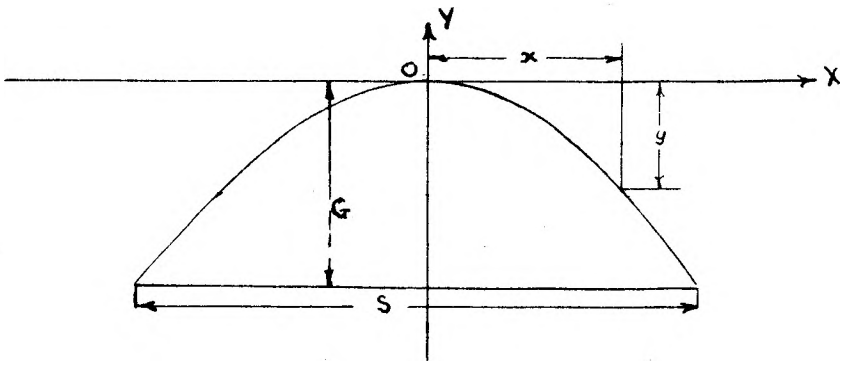

FIGURE (9)

Ideal parabolic arch profile

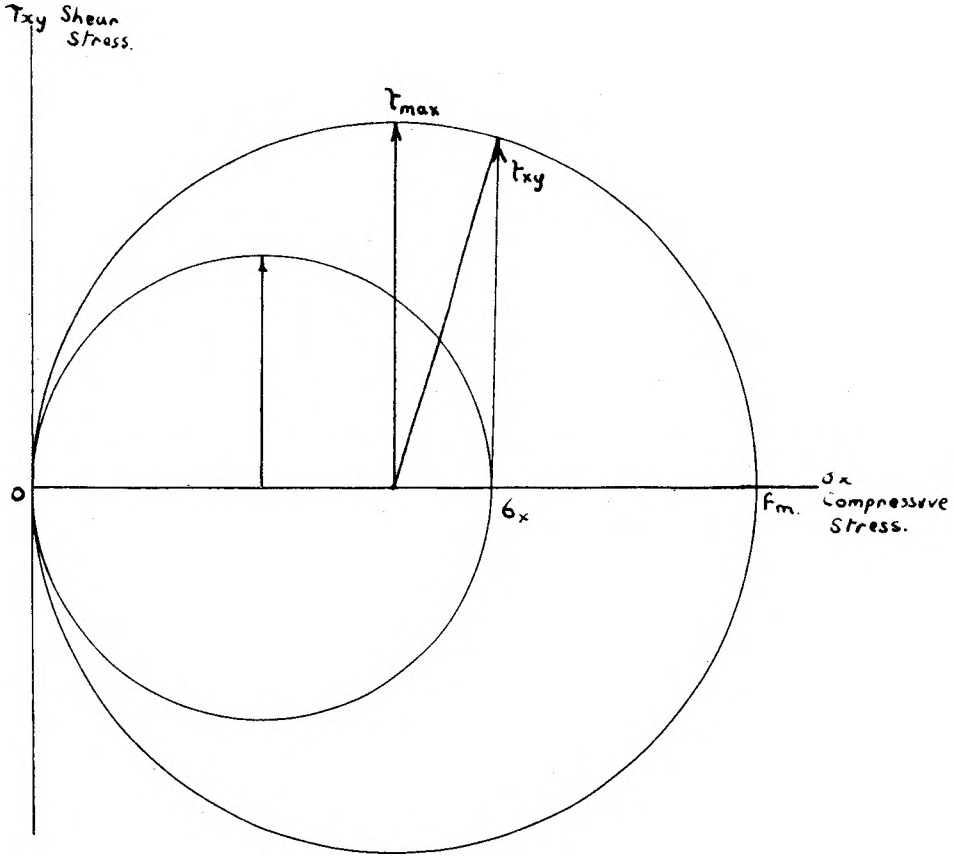

FIGURE (10)

Mohr's circle for abutment stresses

$$\tan \theta = \frac{4\,G}{L} \quad \ldots\ldots\ldots\ldots\ldots\ldots (4)$$

To find the maximum allowable moment of resistance of the beam it is first necessary to find the value of σx, the horizontal stress, in terms of the maximum allowable compressive stress in the arch.

Let the maximum permissible compressive stress in the arch equal f_m. The determination of the principal, stresses at the most critical point in the abutment, from the shear τxy and the horizontal compressive stress σx, is made by means of Mohr's circle as in Figure 10. A circle can be drawn through a point corresponding to the shear and normal stresses acting on a vertical plane at the end of the beam, and at the origin, since there can be no stresses acting on the plane at right angles to the arch line. A circle is shown of diameter $\frac{2\,H}{n\,T}$ or σx, which represents the maximum compressive stress f_m assumed by Evans to be in the beam, neglecting the effect of shear. The maximum shear stress in the former circle, τ_{max}, is the maximum allowable shearing stress of the material, i.e., $2\ \tau_{max} = f_m$.

It is now possible by simple geometry to find the value of σx in terms of f_m and cosine θ. First the value of τ_{max} in terms of σx and τxy must be found. From Figure 10 it can be seen that by the Pythagorian theorem:-

$$\tau_{max}^{\,2} = (\tau xy^2 + (\sigma x - \tau_{max})^2)$$

Therefore $$0 = \tau xy^2 + \sigma x^2 - 2\sigma x\ \tau_{max}$$

$$\tau_{max} = \frac{\tau xy + \sigma x^2}{2\sigma x}$$

But from (3)

$$V = H \tan \theta$$

and it follows that

$$\tau xy = \sigma x \tan \theta$$

Therefore $$\tau_{max} = \frac{\sigma x^2 \tan^2 \theta + \sigma x^2}{2\sigma x}$$

$$\tau_{max} = \frac{\sigma x \ (\mathrm{Tan}^2 \theta + 1)}{2}$$

Now $2 \tau_{max} = f_m$. Therefore

$$f_m = \sigma x \ (\tan^2 \theta + 1)$$

$$\sigma x = f_m \cos^2 \theta \ldots\ldots\ldots\ldots\ldots\ldots(5)$$

From Equation 13 of Evans, (see appendix A) it can be shown that the total moment of resistance is given by the equation:-

$$M = f_m T^2 \left(\frac{n}{2} - \frac{n^2}{6}\right)$$

Therefore it can be seen that only the value of the horizontal stress σx in terms of f_m has been changed, while the remainder of the work is as shown by Evans. The equation of the total moment of resistance becomes therefore:-

$$M = f_m \cos^2 \theta \ T^2 \left(\frac{n}{2} - \frac{n^2}{6}\right) \ldots\ldots(6)$$

From (4) it can be seen that $\tan \theta = \frac{4G}{L}$. Therefore $\cos \theta$ must equal, using the Pythagorian theorem:-

$$\cos \theta = \frac{L}{L^2 - 16\ G^2}$$

Therefore $$\cos^2 \theta = \frac{L^2}{L^2 - 16\ G^2} \ldots\ldots\ldots(7)$$

Substituting equation (7) into (6) gives:-

$$M = f_m T^2 \ \frac{L^2}{L^2 - 16\ G^2} \left(\frac{n}{2} - \frac{n^2}{6}\right)$$

Equating the moment of resistance of the beam to the bending moment we have:-

$$\frac{1}{8} w L^2 T = f_m T^2 \frac{L^2}{L^2 - 16 G^2} \left(\frac{n}{2} - \frac{n^2}{6}\right)$$

The origin of the bending moment is of interest as it takes account of the shear stress present at the end of the beam. From Figure 7 it can be seen that the bending moment is arrived at by taking moments of the weight of the beam and the shear stress at the end of the beam, about the center of the beam. Thus if w be the unit weight density of the beam, then:-

$$\frac{w L}{2} \times \frac{L}{2} - \frac{w L}{4} \times \frac{L}{4} = M$$

Therefore $M = \frac{1}{8} w L^2$

From (8) $$L = \sqrt{\frac{8 f_m T}{w} \left(\frac{n}{2} - \frac{n^2}{6}\right) - 16 G^2} \quad \ldots\ldots\ldots(8)$$

Note that the difference between this equation and the similar equation for the length as given by Evans is in the presence of the $-16 G^2$ term. From the definition by Evans $G = T - \frac{2}{3} n T$, and therefore $T = \frac{G}{1 - 2/3 n}$

Thus $$L = \sqrt{\frac{8 f_m G}{w (1-2/3n)} \left(\frac{n}{2} - \frac{n^2}{6}\right) - 16 G^2} \quad \ldots\ldots(9)$$

The effect of deflection of the arch under load is now considered. This deflection is only a critical factor on thinner beams as discussed by Evans. For the higher arches the accuracy achieved by allowing for deflection is not warrented as the problem at best is inherently only an approximation. Abutment strain in a horizontal direction is shown by Evans

to have little or no effect on arch stability, and it follows that abutment deflection in a vertical direction, like the deflection in the arch itself, has a negligible effect on the overall behavior of the system.

In massive rock the height of an arch is limited only by the physical characteristics of the material in which it acts, and the width of the initial undercut, i.e., not by the thickness of strata as is the case in bedded deposits. The height to which an arch develops under a given set of conditions depends upon the superincumbent load, the strength of the rock and the width of the opening. Arch height can be calculated from (8), putting the effect of the overburden into the equation by increasing the effective density of the material.

Thus let w be the normal unit weight, and w_2 the effective unit weight. If h is the depth of the beam plus overburden, then:-

$$w\ h = w_2\ G$$

Therefore $$w_2 = \frac{w\ h}{G} \quad \ldots\ldots\ldots\ldots\ldots (10)$$

Putting (9) into (8) we have:-

$$L = \sqrt{\frac{8\ f_m\ G^2}{wh\ (1-2/3n)} \left(\frac{n}{2} - \frac{n^2}{6}\right) - 16\ G^2}$$

Solving for G we have:-

$$G = \frac{L}{\sqrt{\frac{8\ f_m}{wh(1-2/3n)} \left(\frac{n}{2} - \frac{n^2}{6}\right) - 16}} \quad \ldots\ldots (11)$$

In practice the effect of the overburden load is not instanta-

neous with the removal of the undercut, and the weight of the entire overburden is felt only after a period of time that may stretch into years. Thus a time factor which varies with the rock concerned, and whose value can only be ascertained from the prototype, must be allowed for in all caving or doming calculations.

CHAPTER IV

EXPERIMENTAL INVESTIGATION OF THE MECHANICS OF BLOCK CAVING

Introduction

Due to the complex stress conditions prevailing around irregularly shaped mine openings, it was concluded that the problem of block caving would be most amenable to stress analysis using photoelastic techniques. Testing to failure, using models of a brittle material, loaded by body forces might also have yielded valuable experimental data, but the difficulties inherent in producing uniform stress fields in such models creates problems which do not appear soluble at the present time.

Equipment

With the exception of the model holder, no special equipment was developed for these tests, although the apparatus did include the use of a large centrifuge constructed specifically for the testing of models.

The centrifuge has a rotor diameter of six feet and is capable of developing 2,000 'g's at 1,500 r.p.m, see plate 1 . To minimize air resistance on the rotor, it is encased in an air tight steel shell, capable of being evacuated to one inch of mercury on a S.T.P. day. The centrifuge was powered by a ten horse power, D.C. shunt

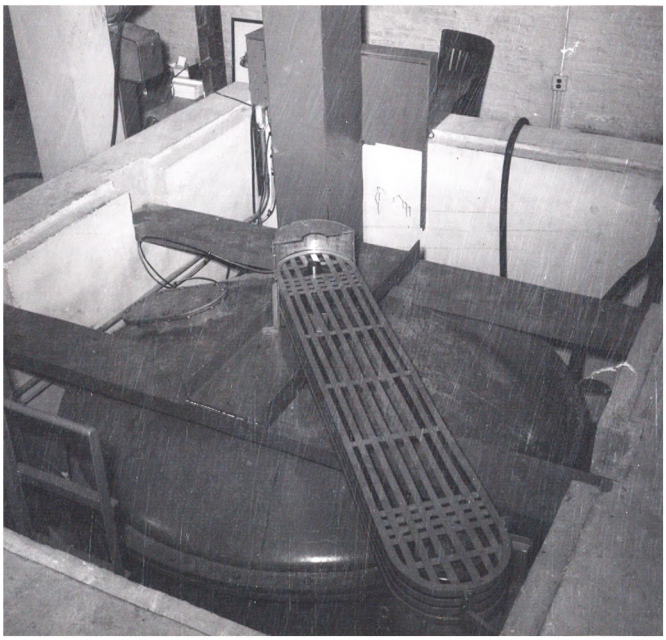

Plate 1 Centrifuge

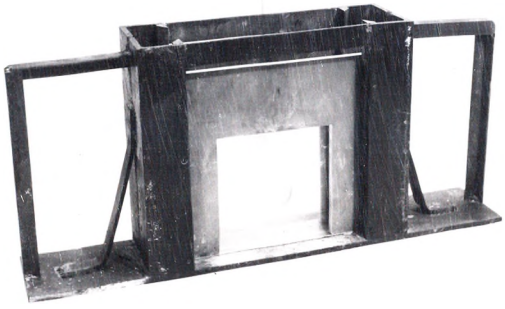

Plate 2 Model Holder

wound motor consuming 240 volts at 38.3 amps. The D. C. power source was a ten horse power motor generator set, while the vacumn was created by an Ingersoll-Rand Type 30 vacumn pump.

The models were examined in a standard type polariscope using eight inch polaroid plates. Both white and monochromatic light sources were used.

The model holder was constructed so as to give lateral support to the model during the test. The holder was constructed of steel and the model was supported in the holder by wooden blocks, and wedges. (See plate 2 .)

Model Construction

To facilitate the use of the centrifuge as a source of model body forces, a modified stress freezing technique as suggested by Dally, et al, was used. The strains were frozen in the model while under centrifugal load, and thus the model did not have to be examined while in the centrifuge. A clear epoxy resin called Araldite 502 was used in the construction of the model, mixed with a plasticiser and an Araldite hardener to give the desired material properties. A standard mixture was used in all tests, as was suggested by Dally. This mix was:-

Araldite 502	72%
Dibutyl Phthalate	20%
Hardener, HN951	8%

If it had been required, the modulus of elasticity could have been varied by altering the quantity of plasticiser used in the mixture.

The models were allowed to cure for 12 hours before being subjected to load, and then a final four hours was needed before the curing process was complete. During the latter four hours, the model was under load in the centrifuge.

Dally suggested that the models should be cast in an aluminum mold and placed in a cooling water bath, during the initial stages of curing to remove the heat generated in the exothermic reaction. This was, however, found to be unnecessary and the models were poured in lucite molds that needed no mold release agent, since the models were relatively thin and did not have to be cooled.

Model Loading

As the models were relatively thin and had to be subjected to a lateral load in addition to the centrifugal body forces, a special model holder was used to hold the models in place during the tests. To prevent buckling, the model was held between two lucite sheets that had been greased to reduce friction. These were found to have no effect on the fringe distribution within the model. Lateral support was given by means of wedges placed against the ends of the model that could be used to fill in the spaces between the model

PLAN.

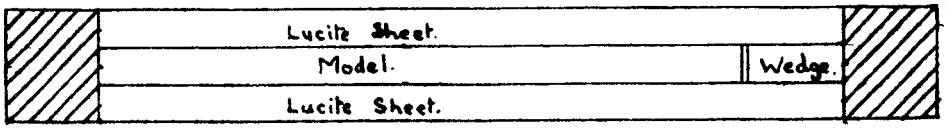

SECTION.

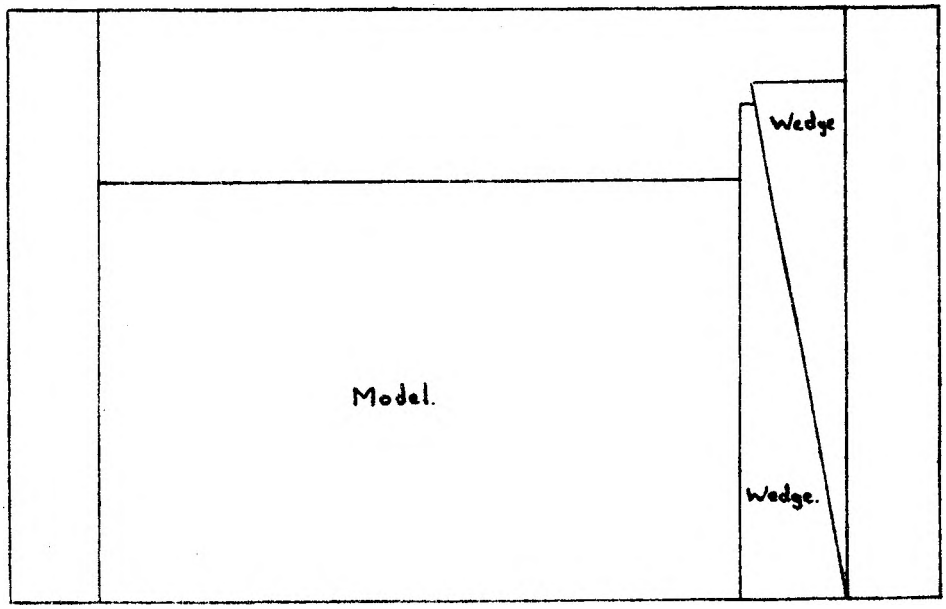

FIGURE (11)

Model support arrangement

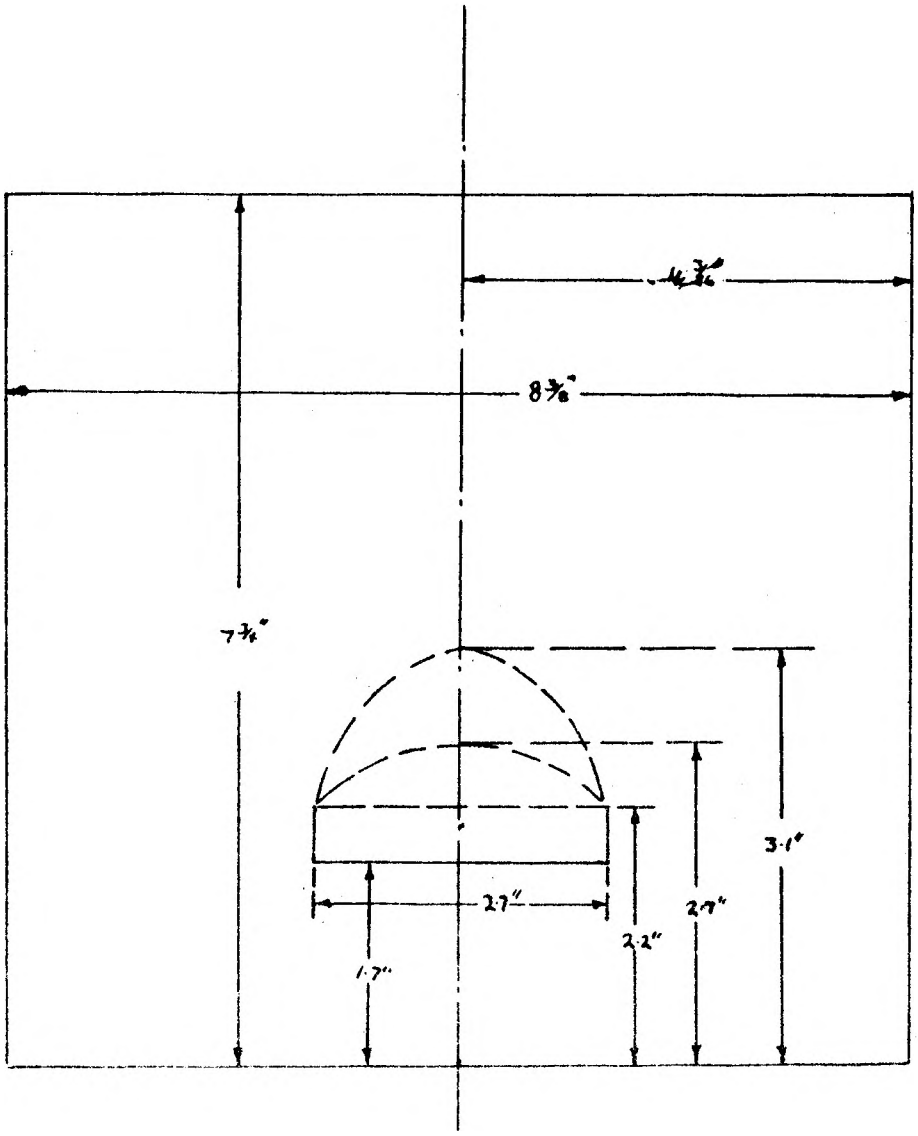

FIGURE (12)

Model dimensions

and the holder. (See Figure 11.) No lateral pressures were applied to the model prior to loading, but expansion of the model in a lateral dimension was prevented while under load. Thus the lateral pressure produced was due to the lateral restraint, the effect of which was determined by making a calibration test of a round opening in a plate. The stress concentrations around a circular opening in various types of stress field were known, Duvall[16] and a comparison of the stress concentrations around the test model with the results as given by Duvall gave the value of the lateral stress field.

Model Dimensions

The models were constructed as thin plates with the object of representing stress distributions across a section of the prototype. That is, models subjected to plane stress conditions, were used to simulate prototypes whose loading conditions approximate plane strain. Pertinent dimensions of all models are shown in Figure 12.

Model Calibration

All the tests were carried out under identical conditions, using the same epoxy material. The value of the modulus of elasticity and the photoelastic constant were identical for all tests, although their values were not required for examination of the models, as direct comparisons of fringe orders could be made when comparing stresses

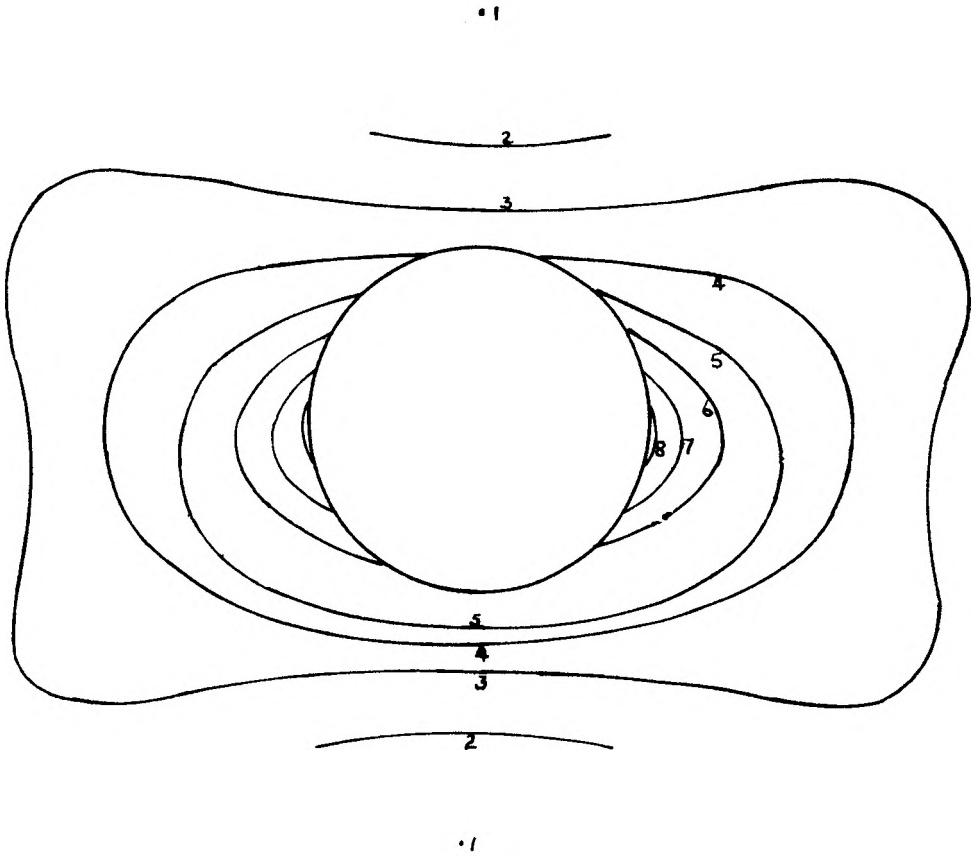

FIGURE (13)

Calibration test stress distribution

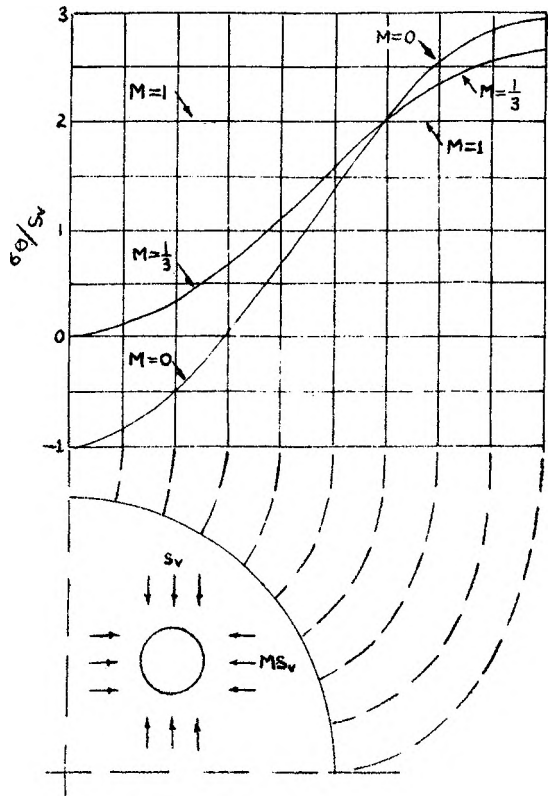

FIGURE (14)

Boundary stress concentration for a circular opening

from model to model. Since the models were tested within their elastic limits, the shape of the model was geometrically the same as the prototype. (Assuming it also was within its elastic limit.)

For the estimation of the lateral pressure developed within the model a test was run on a circular opening in a plate loaded by centripetal acceleration. The resulting monochromatic fringes at the top and bottom were of different value. This was due to the combined effect of the bottom of the model being subjected to a greater centripetal acceleration than the top, and the fact that it had more material above it. A good approximation is achieved by taking the mean of these two results, thus the ratio of the average of the maximum stress at the top and bottom of the opening to the sides is:-

$$\frac{\frac{4.5 + 5.5}{2}}{8} = 0.562$$

From the work of Duvall, see Figure 14, it can be seen that when the ratio of the stresses at the sides and top of an opening is 0.562, and the plate is laterally restrained, the value of Poisson's ratio is 0.398. This result agrees closely with the value of 0.367 to 0.465 given by Dally.

Model Tests and Results

To examine the stress distribution around a series of differently shaped mine openings, four tests were run.

Plate 3 Stress Pattern in Test 1

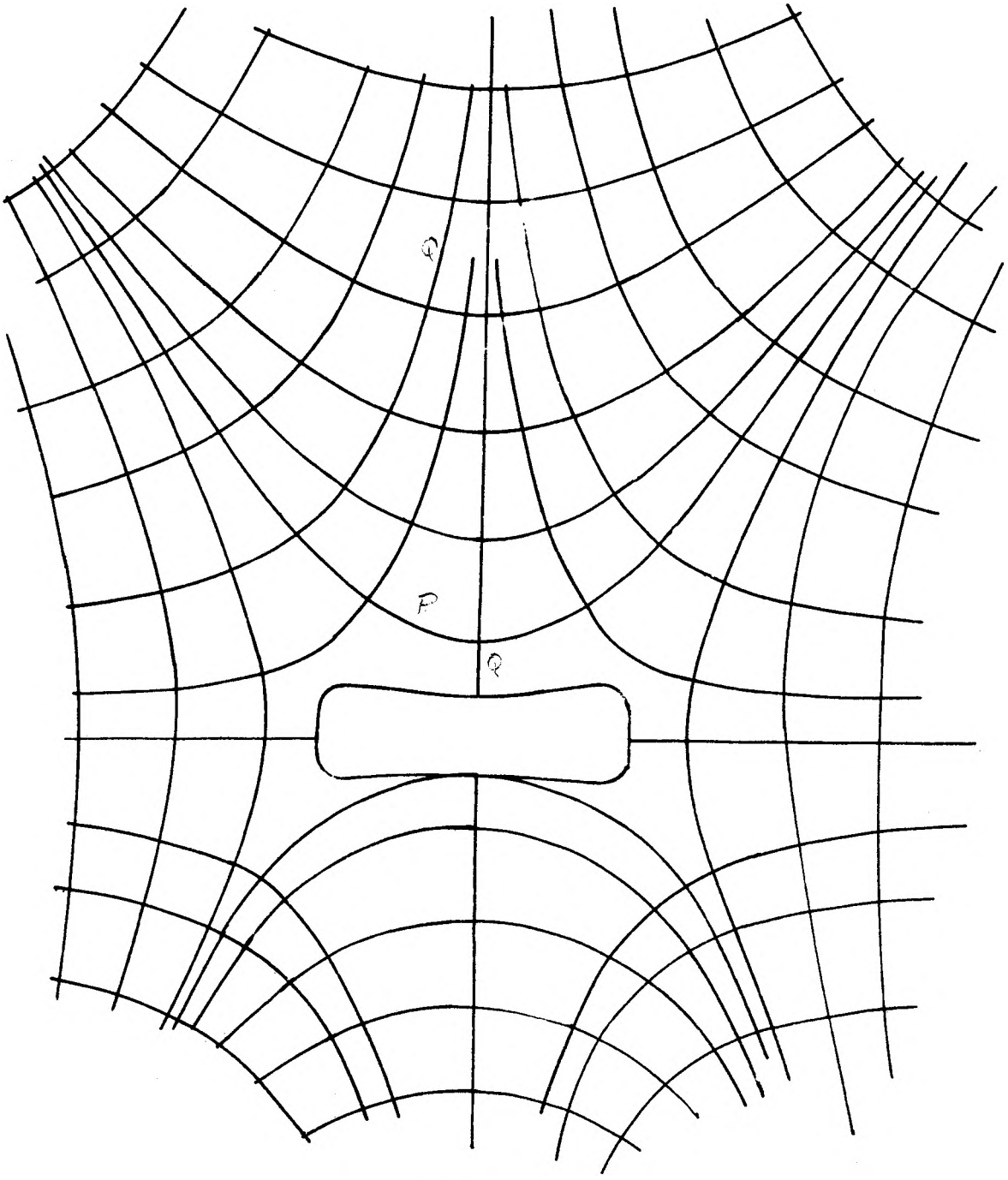

FIGURE (15)

Stress trajectories in model 1

Plate 4 Stress Pattern in Test 2

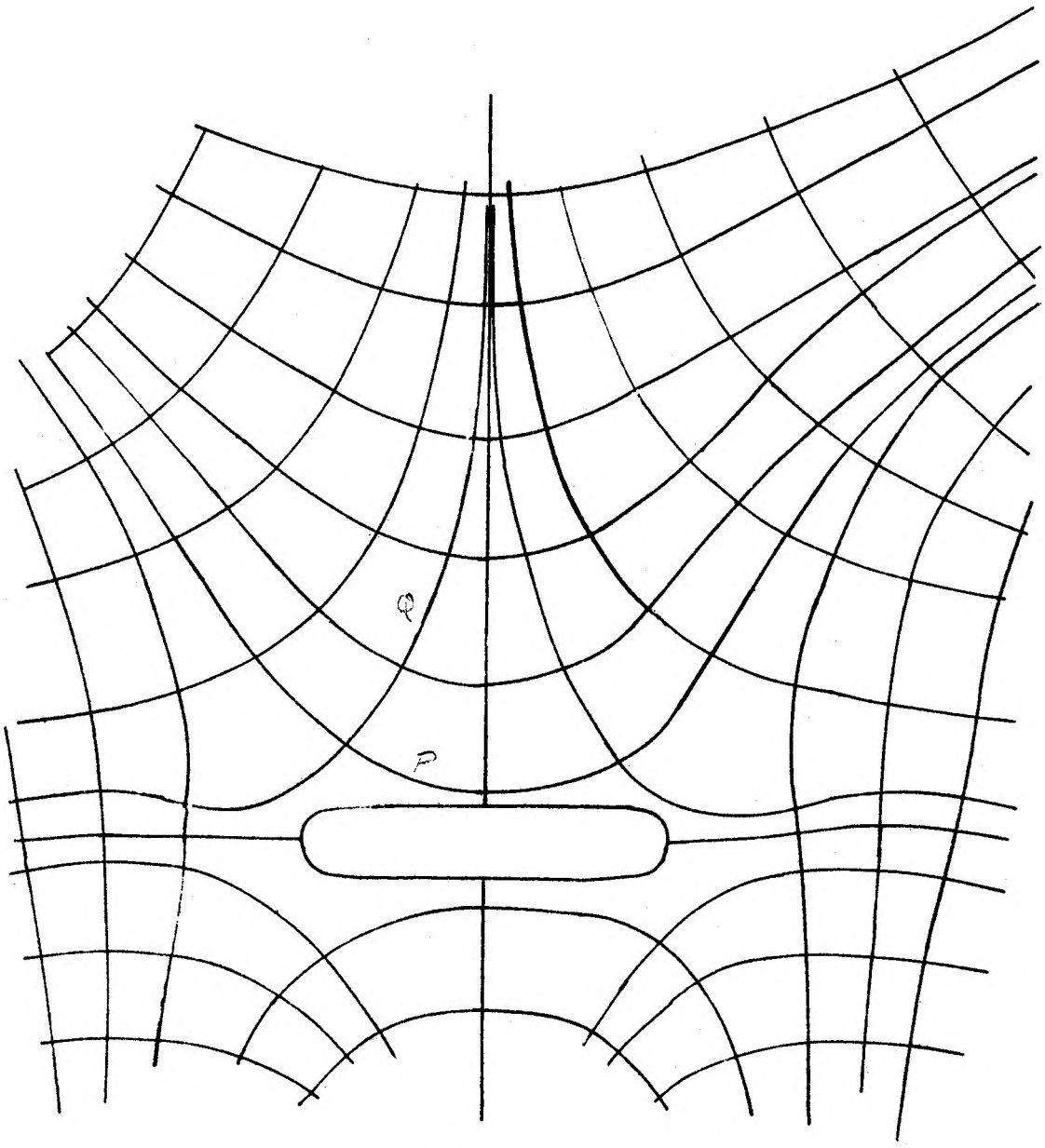

FIGURE (16)

Stress trajectories in model 2

TEST 1.

The purpose of this test was to determine the stress distribution around a simple rectangular opening with rounded corners, in a plate loaded by centrifugal body forces. The test was conducted with lateral restraint being applied to the model, the lateral force being approximately equal to 0.6 (as taken from the calibration test.) of the applied vertical force. The test results are shown in plate 3 . Stress trajectories are shown in figure 15.

TEST 2.

This test was conducted on an opening shaped as in test one, but in this case, smooth, plain cuts had been placed in the model as shown in figure 16. As a result, the top of the opening could support itself neither as a simple beam nor in any cantilever type arrangement, and therefore, had to develop an arch structure to maintain stability. Test conditions were the same as in test one. The resulting fringes are shown in plate 4 , and the stress trajectories in figure16 . It was observed in this model that the vertical cut had opened to some distance above the opening, showing, definitely that this part of the model was under tension. The cuts on either side of the opening seemed unaffected by the test.

TEST 3.

This test was conducted under the same test conditions as test 1 and 2, though in this case the shape of the open-

Plate 5 Stress Pattern in Test 3

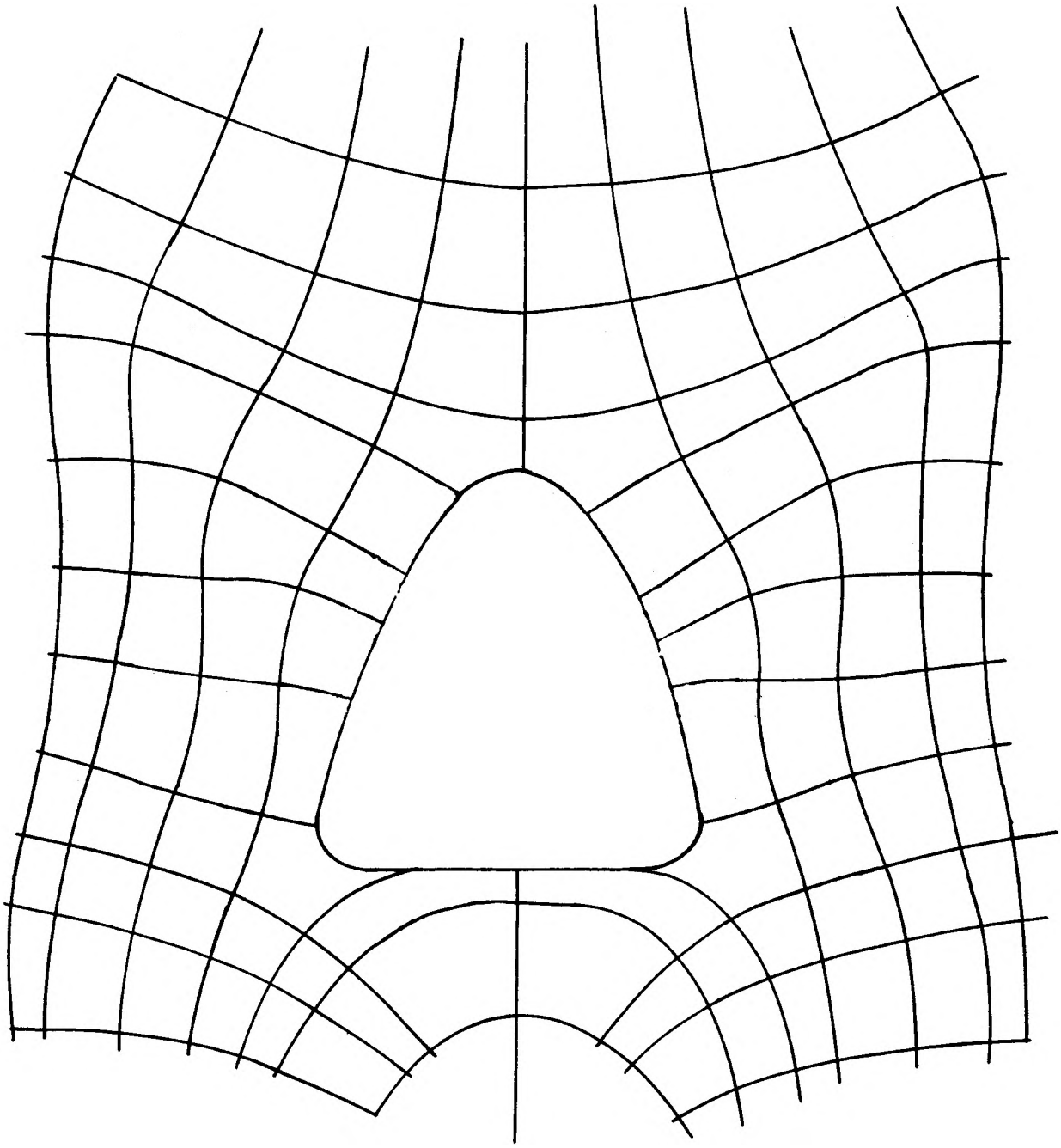

FIGURE (17)

Stress trajectories in model 3

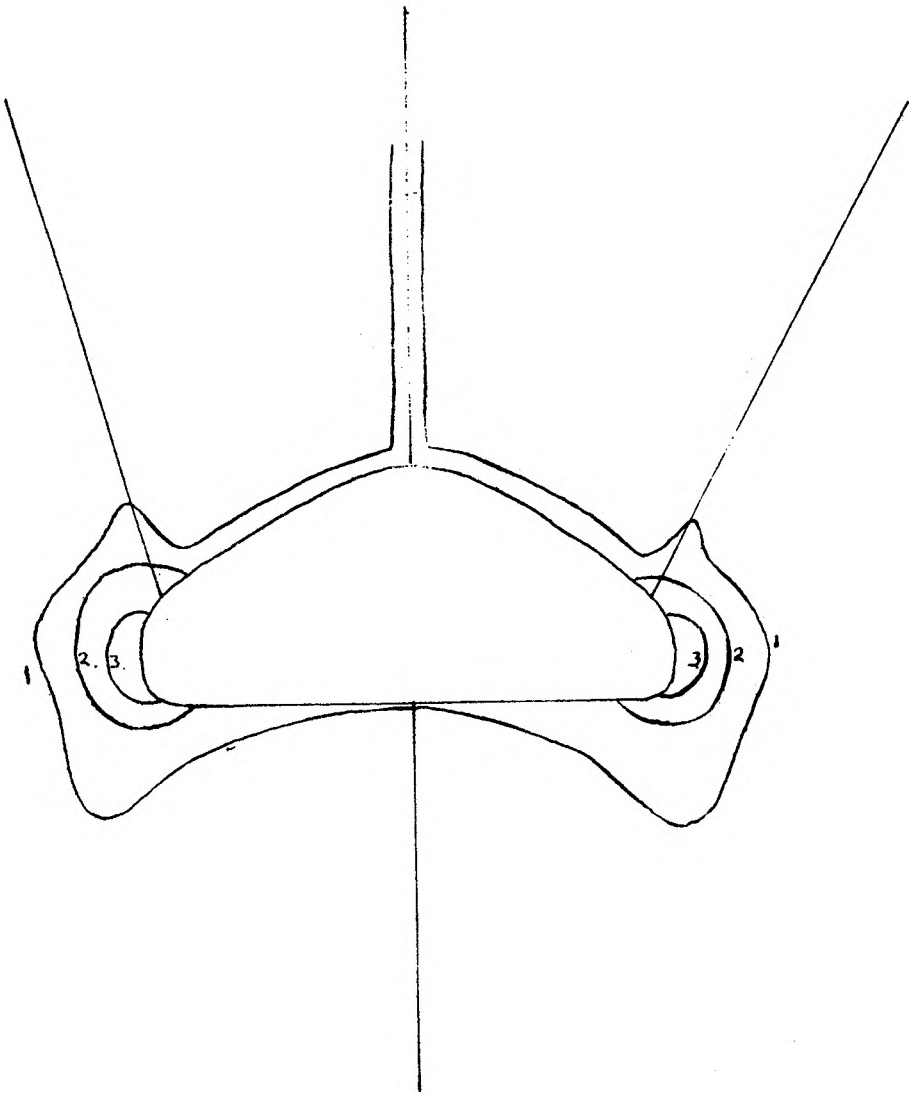

FIGURE (18)

Stress pattern in test 4

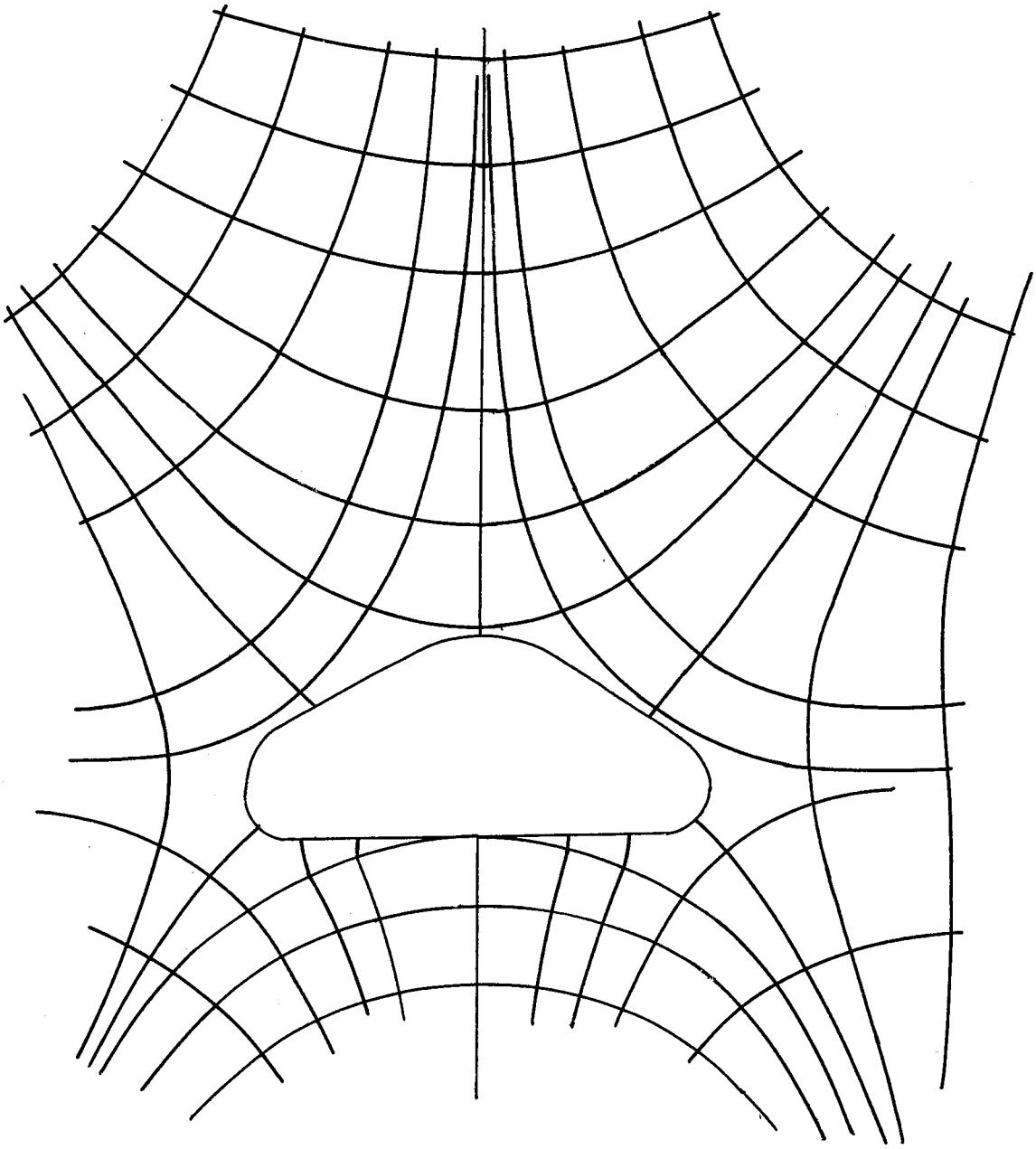

FIGURE (19)

Stress trajectories in model 4

ing was changed. For this test a semi-parabolic opening, as shown in figure 17 , was used with cuts placed as in test 2. Loading across the span of the opening due to the weight of the overlying material was not uniform, but the opening was made small to try and minimize the effects that this might have on the stress distribution. The results of this test can be seen in plate 5 and the stress trajectories in figure 17 . No tension separations were observed in this model in any of the plane cuts.

TEST 4.

Test conditions in this test were the same as in previous tests and a parabolic opening was used again, with an overall height less than in test 3. Results of this test are shown in figure 18 and the stress trajectories in figure 19. In this model the vertical cut had opened showing that this part of the model was subjected to a tensile force.

CHAPTER V

ANALYSIS OF RESULTS

Results of Theoretical Investigation

The theoretical development of the theory of the Voussoir beam shows that as the arch height increases, the shear stress, and correspondingly the principal compressive stress at the abutment, increases. Figure 20 represents plots of beam length versus thickness at the point of instability, derived using the equation by Evans (4) and that developed by the author (9) as shown below.

For both equations the following substitutions were performed.

T = thickness of the beam.

L = length of arch span.

w = 156 pounds per cubic foot.

f_m = 2,240 p.s.i.

n = 0.5.

The point (a) on the curve after Evans was obtained as follows:-

$$L = \sqrt{\frac{8\ f_m\ T}{w}\left(\frac{n}{2} - \frac{n^2}{6}\right)} \qquad \text{.....(13)}$$

$$L = \sqrt{\frac{8 \times 2240 \times 144\ 100}{156}\left(\frac{1}{4} - \frac{1}{24}\right)}$$

Therefore L = 575 feet.

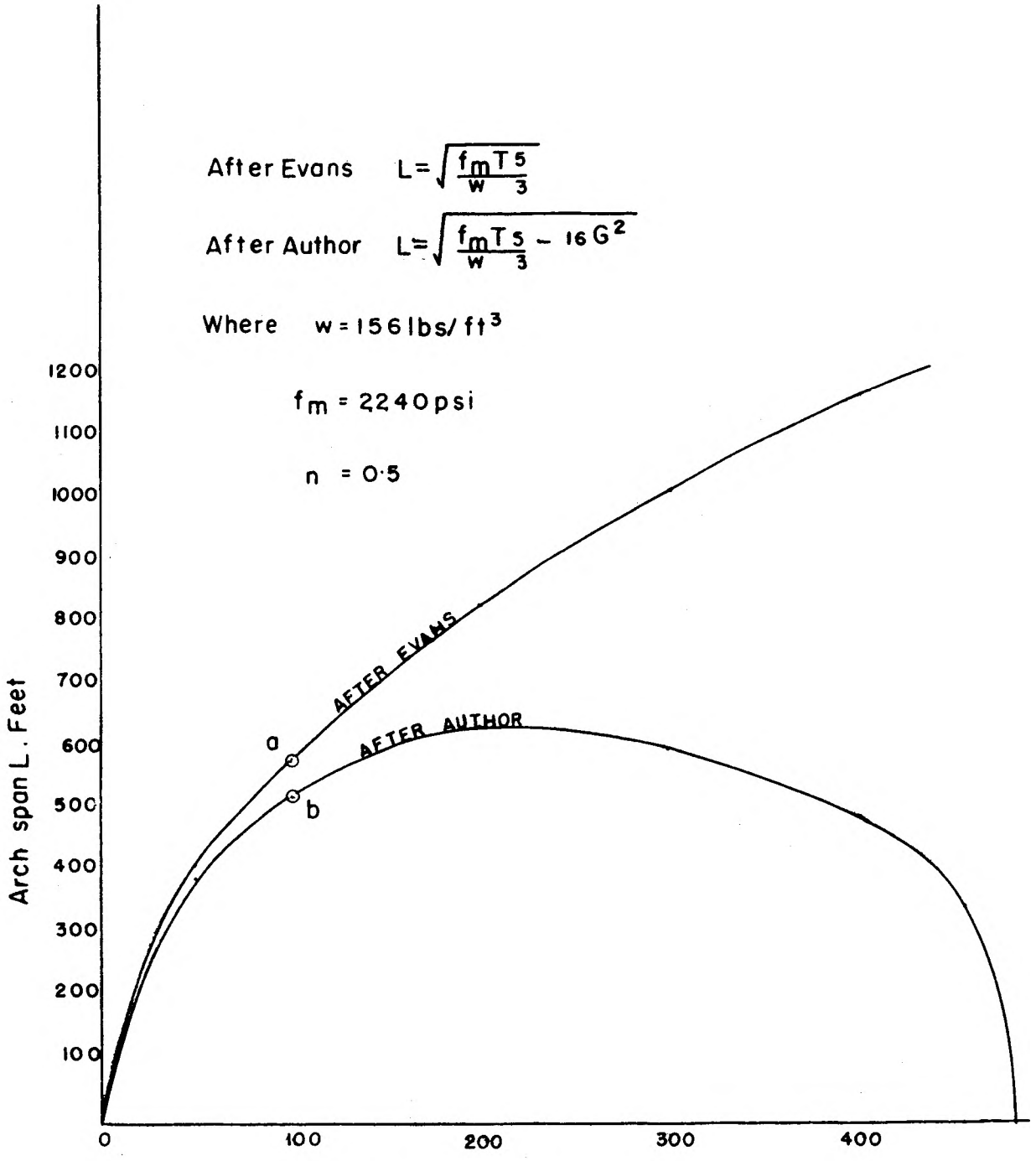

FIGURE (20)

Curves of Voussoir arch span vs. beam thickness

In the case of point (b) on the author's curve

$$L = \sqrt{\frac{8\, f_m\, T}{w}\left(\frac{n}{2} - \frac{n^2}{6}\right) - 16\, G^2} \qquad \ldots\ldots\ldots (9)$$

It was assumed in the derivation of ( ), that for the case, $G = T - 2/3\, nt$

Therefore $G = 100 - 2/3\,(0.5)(100)$

$$G = 66.67$$

and
$$L = \sqrt{\frac{8 \times 2240 \times 144 \times 100}{156}\left(\frac{1}{4} - \frac{1}{24}\right) - 16 \times 66.67^2}$$

$$L = 521 \text{ feet.}$$

It can be seen that the effect of the shear stress component on the critical dimensions of the arch, becomes appreciable only as the arch height increases considerably. This would be true particularly in the case of weak rock, since in equation (9) the contribution of the term including f_m would become relatively smaller or for long spans, when the term including G, the arch height necessarily becomes large. As can be seen from the lower curve in figure 20, the effective span L of the beam reaches a maximum value as the thickness of the beam increases. The maximum possible height is independent of the length of the beam and can be found by equating the terms under the radical sign in equation (9), and letting $n = 0.5$.

$$8 \times \frac{5\, f_m\, T}{24\, w} = 16\, G^2_{max}$$

But as stated by Evans $T = \dfrac{G}{1 - 2/3n}$

Therefore the expression for maximum arch height becomes,

$$G_{max} = \frac{5\ f_m}{48\ w\ (1 - 2/3n)}$$

When n = 0.5 the expression becomes:-

$$G_{max} = \frac{5\ f_m}{32\ w}$$

In contrast, the curve representing Evans's equation (14) predicts that the length of the span would increase indefinitely as the thickness T of the strata increased. Inclusion of the shear stress component in the resultant stress at the abutment leads to the prediction, in cases where the arch height is large, that failure would be most likely to occur at the abutment, rather than at the top of the arch. In the case put forward by Evans, failure could occur at either of these two places, since the stresses were assumed equal at both points.

Consideration of the effect of overburden indicated that a minimum arch height for stability exists in massive rock under any given set of conditions, as can be seen from equation(11), i.e.,

$$G = \sqrt{\frac{8\ f_m}{w\ h\ (1 - 2/3n)} \left(\frac{n}{2} - \frac{n^2}{6}\right)^{-1} - 16} \quad \text{.....(11)}$$

At the point where the arch is just stable an increase in stability can be achieved by increasing the arch height, assuming all other factors remain constant. In this case, it is presumed that the entire weight of the overburden above the opening is thrown onto the arch. This might not be completely true in practice, as the rock composing the

overburden would probably have some tensile strength, and large fragments might act in a cantilever fashion to support some of the load. Nevertheless, the assumption is not completely unwarrented, as in highly fractured ground rock has a tendency to flow, as does broken material in a shrinkage stope.

The gradual settlement of the overburden composed of broken rock explains the time factor present in block caving and is seemingly dependent on the ability of the material to flow or settle.

Consideration of equationll shows that the arch height would go to infinity when the left hand term under the square root system equals 16. This would be the case either when f_m was very small or under great depths of overburden, h; i.e., if the rock had a compressive strength of 2,000 p.s.i., the arch height would become infinite if the depth were:-

$$h_{max} = \frac{8\ f_m}{w\ 16\ (1 - 2/3n)} \left(\frac{n}{2} - \frac{n^2}{6}\right)$$

or $$h_{max} = \frac{5\ f_m}{32\ w} \qquad \text{when } n = 0.5$$

$$h = \frac{8 \times 2{,}000 \times 144}{150 \times 16\ (1 - 2/3 \times 1/2)} \left(\frac{1}{4} - \frac{1}{24}\right)$$

$$h = 300 \text{ feet.}$$

Thus if the undercut were at a depth greater than 300 feet, ultimately the caving would continue to the surface.

If an undercut were to be put in at 200 feet below the surface and it was desired that it should break through to the surface the arch height required would be 300 feet, or greater. Therefore, if conditions were the same as for the previous example, the minimum length of the undercut would be, using equation(11)* -

$$L = 200 \sqrt{\frac{8 \times 2{,}000 \times 144 \times 3 \times 5}{200 \times 150 \times 2 \times 24}} - 16$$

$$L = 564 \text{ feet.}$$

This dimension may appear somewhat large, due to the low depth at which the excavation was to have been made. In practice such a proposed cave would probably require boundary weakening stopes or drifts.

Results of Experimental Investigations

The first photoelastic model test of a rectangular opening showed that the ground immediately above an opening contains tensile stresses that may be the cause of the initial failure of the opening. The stress trajectories indicated that the vertical stress had been shunted to the side, although the model was not of sufficient lateral extent to determine whether this effect extends a large distance beyond the opening.

The second model, a rectangular opening with tensile stress relieving cuts demonstrated that the tensile stress observed in test one could cause failure at the top of the opening as shown by the widening of the saw cut at that

point. Since there could not have been any cantilever effect, due to the presence of saw cuts at the edges of the opening, the material above the opening must have been supported by an arching action. The stress trajectories illustrated that the vertical load was thrown to the side of the model but maintains a vertical component. The apparent lateral extent of the arching effect was much greater than might be expected though this may have been due to the model support conditions.

In the third test the opening was semi-parabolic and the resultin fringe distributions established the fact that only the compressive stresses were acting around the opening, as in the case of a true arch. However, the high stress concentration at the top of the opening indicates that some material which would have normally carried compressive stresses across the arch was removed. The arch height in this case was above that of a natural arch for these conditions. The stress trajectories were somewhat similar to those of test two.

The fourth model, consisting of a flattened parabolic opening, gave results sililar to those in test one, as tensile forces had opened the saw cut at the top of the arch. Stress trajectories were similar to those from test three, although the arch height was obviously below that of the natural arch height. This was a case of an underdeveloped arch, an it is of interest to note that the initial limits of the arch were controlled by the vertical extent of the

tension cracks forming at the top of the opening. That is, the point where crack separation above the model is no longer apparent may be taken as the lower limit of the arch.

CHAPTER VI

CONCLUSIONS

It has been shown that the shear stress component of the resultant force at the abutment in a Voussoir arch is a major factor in determining the stability of the arch, when the arch height becomes large in respect to the width of the opening. The effect of the shear stress component is to limit the height to which an arch can form above a mine opening, irrespective of the thickness or length of the beam in which it forms. The maximum stable arch height based on this premise can be approximated by the expression:-

$$C_{max} = \frac{5\ f_m}{32\ w} \quad \text{where n is taken to be 0.5.}$$

This in contrast to the work by W. H. Evans, who predicted that as the width of the opening increased, the arch height for stability would also increase, without limits. In high arches, failure is most likely to occur at the abutment due to the high stress concentration there, rather than at either the top or abutment of the arch, as predicted by W. H. Evans.

In those cases, where a Voussoir beam is covered by an incompetent layer, a definite relationship has been established between the compressive strength of the rock composing the Voussoir beam, the unit weight of the overburden and the limiting height of the beam plus overburden, independent

of width of opening and arch height. That is the maximum height of overburden plus beam thickness which can be supported by a Voussoir beam may be approximated by the expression:-

$$h_{max} = \frac{5\ f_m}{32\ w} \quad \text{when n is taken to be 0.5.}$$

From the model studies it was demonstrated that tensile failure in the top of the opening is the initial cause of failure. Thus neither tensile strength nor cantilever action provides the support for heavily fractured ground, and only arching of the ground above the opening can maintain the stability of the opening. An arch can form only when there is sufficient lateral support to maintain it. The initial height of the arch is determined by the effective vertical extent of tensile stresses and associated fractures.

From the data presented it has been shown that a dome probably exists above underground openings, where either the tensile strength of the rock has been exceeded, or the rock was prefractured and can carry no tensile stresses. The dimensions of the dome depend upon the characteristics of the rock concerned, and the size of the undercut opening.

A proposal is now put forward as to the mechanics of failure of the ground in a caving block. Immediately after undercutting the roof begins to move downward behaving as a simple beam. Tension cracks form at the center of the undercut and extend upwards. As the material continues to move downward it tends to pivot about the abutments, and as

this movement is limited, the load is thrown across the top of the opening in the form of a natural arch. The low tensile strength of the rock causes most of the material below the arch line to fail and fall away. Initially if the arch height is low, it may be instable. As a result compressive failure will occur at the abutments or the top of the arch, as predicted by W. H. Evans as the weight of the overburden settles upon it. As the dome height increases, and if the dome still is not stable, failure will occur at the abutments and the dome will increase in height in an effort to become stable. Material below the arch line will fail as previously mentioned.

This hypothesis can only be a very crude approximation of what happens in actual fact. The many variations in rock characteristics, fracture patterns, etc., makes a completely accurate statement impossible. However it is hoped that the mechanics of the Voussoir arch may provide some basis for a quantitative analysis of large underground openings in massive rock, and an estimation of the probable stability of such openings.

For further study of the mechanics of block caving using the theory of the Voussoir arch, it is recommended that the effect of loss of material below the arch line be investigated, as this might affect the present estimates of the limits of stability calculated with the material in place. Brittle models could be used to show actual failure of the

ground above openings, and the points of failure in actual artificially constructed arches. The photoelastic study contained in this thesis could be enlarged by considering, the effects of variation in lateral pressures, and of the influence of boundary weakening systems. A model constructed of blocks of a photoelastic material might also yield valuable results as this would ensure that no tensile stresses were present in the model at any point, as would be the case in the prototype.

BIBLIOGRAPHY

1. Bucky, P. B. (1956) "Mining by Block Caving". Colorado School of Mines Quarterly, Vol. 51, No. 3, p. 129-143.

2. Isaacson, E. de St. Q. (1958) Rock Pressure in Mines, London, Mining Publications Ltd. p. 209.

3. Fletcher, J. B. (1959) "Ground Movement and Subsidence from Block Caving at Miami Mine", Soc. of Mining Eng. Preprint No. 59AU27, p. 28.

4. Woodruff, S. D. (1960) "Rock Mechanics of Block Caving Operations", Intern. Symposium on Mining Research, University of Missouri, School of Mines and Metallurgy. Pergamon, London. p. 509-520.

5. Shoemaker, R. P. (1951) A review of rock pressure problems. Colorado School of Mines Quarterly. Vol. 46, No. 1. p. 127-144.

6. Fenner, R. (1938) Untersuchungen zur Erkenntniss des Gebirgsdrucks. Gluckauf, n. 32, p. 681-695, n.33., p. 705-715.

7. Denkhaus, H. G. (1958) The application of the mathematical theory of elasticity to problems of stress in hard rock at great depth. Assoc. of Mine Managers of South Africa. Papers and Discussions, 1958-1959. p. 271-309.

8. Irving, C. J. (1946) Some aspects of ground movement. Journal of the Chem. Metallurgucal and Mining Soc. of South Africa. Vol, 46. p. 278-312.

9. Mohr, F. (1956) Influence of mining on strata, Mine and Quarry Eng., Vol. 22.

10. Dinsdale, J. R. (1937) Ground failure around excavations. Transactions of the Institute of Mining and Metallurgy. Vol. 46. p. 673-687.

11. Evans, W. H. (1941) The strength of undermined strata. Transactions of the Instutute of Mining and Metallurgy. Vol. 50, p. 475-532.

12. Manning, G. P. (1954) Reinforced concrete arch design. 2nd. ed. Sir Isaac Pitman and Sons, Ltd. London p. 1-11.

13. Hetenyi, M. (1950) Handbook of experimental stress analysis. Wiley, New York. p. 663-699.

14. Frocht, M. M. (1941) Photoelasticity. Wiley, New York. Vol. 1. p. 401.

15. Dally, J. W., Durelli, A. J., Riley, W. F. (1957) Journal of Applied Mechanics. Paper N. 57-A 71. p. 1-7.

16. Obert, L., Duvall, W. I., Merill, R. H. (1960) Design of underground openings in competent rock. Bulletin 587, U.S.B.M. p. 36.

APPENDIX A

A review of the mechanics of the Voussoir arch as applied to massive strata, as proposed by W. H. Evans[11], is presented here.

The limitations and assumptions applied to the problem by Evans may be found in Chapter III on Theoretical Investigations. His derivation of the total moment of resistance illustrated in figure 21, is presented here.

Let T = thickness of the beam.

nT = depth of section under horizontal compressive stress.

$\frac{1nT}{3}$ = distance of line of thrust from beam surface.

Hence G = arm of couple.

$= T - 2((1/3)nT)$

$= T\ (1-(2/3)nT)$

Let H = thrust.

$= \frac{f_m}{2}$ x nT per unit width; f_m = maximum allowable stress.

The moment of resistance m_2 due to horizontal thrust at the ends equals:-

$$m_2 = H \times Z.$$

$$= \frac{n}{2} \cdot f_m T \times T\ (1 - 2/3n)$$

$$= f_m \cdot T^2 \cdot \frac{n}{2} - f_m T^2 \frac{n^2}{3}$$

$$= f_m T^2 \left(\frac{n}{2} - \frac{n^2}{6}\right) \quad \ldots\ldots\ldots\ldots\ldots\ldots (12)$$

To obtain the end fixing moments, it is assumed that a

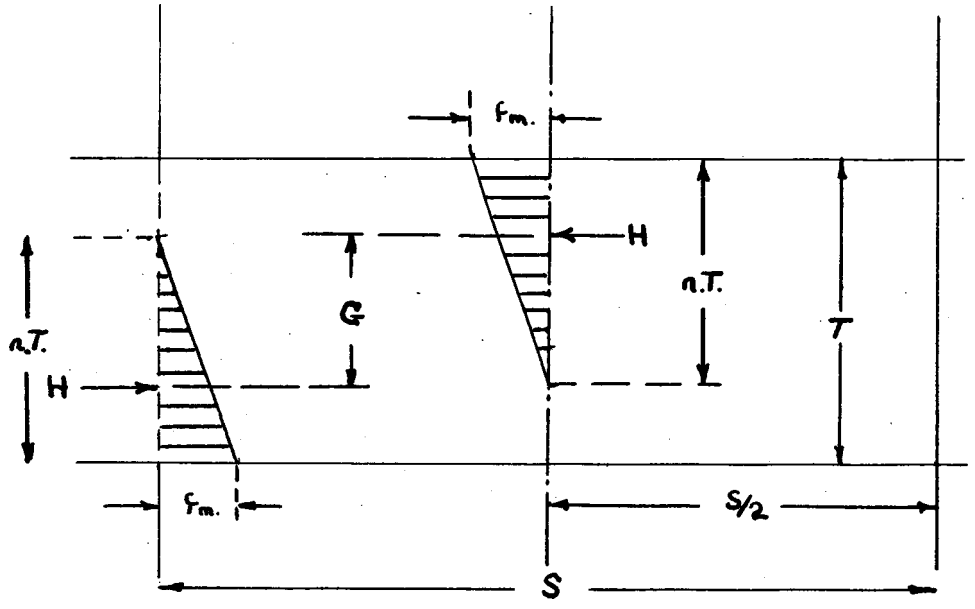

FIGURE 21

Force distribution in a Voussoir beam, after Evans

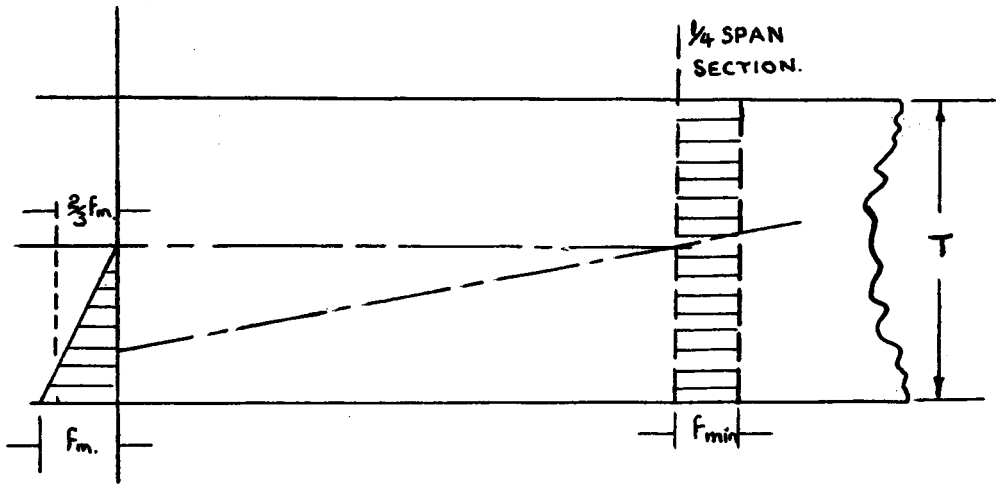

FIGURE 22

Distribution of compressive stress along the arch line, after Evans

moment m_3 is induced at each end of the beam, because the center of thrust does not coincide with the center of area under compression:-

$$H = \frac{f_m}{2} \; nT \text{ as before.}$$

$\frac{n\,T}{6}$ = its eccentricity.

Therefore $$m_3 = \frac{f_m \times n^2 \, T^2}{12}$$

Strength due to simple bending can be determined. The line of thrust that acted eccentrically to the center area at the end of the beam, also acts eccentrically at the center of span, and induces another moment of resistance there. As can be seen from figure 21 the moment m_1 is equal to m_3 by the symmetry of the figure.

Hence the total moment of resistance M is written:-

$$M = m_1 + m_2 + m_3 = f_m \, T^2 \left(\frac{n}{2} - \frac{n^2}{6}\right) \ldots\ldots\ldots (13)$$

A convenient figure of n = 0.5 may be taken, giving optimum strength of the average strata in underground conditions.

Therefore $$M = \frac{5}{24} \; f_m \, T^2$$

Equating the bending moment to the total moment of resistance gives:-

$$\frac{1}{8} \, w \, L^2 \, T = \frac{5}{24} \, f_m \, T^2$$

$$L^2 = \frac{5}{3} \, \frac{f_m \, T}{w}$$

$$L = \sqrt{\frac{5}{3} \, \frac{f_m \, T}{w}}$$

Effect of Deflection

Deflection causes reduction in the arch height, and therefore equation (14) must be modified. Deflection may have two sources, bending moments, and compression along the arch line. The former may be taken to be negligible and only the latter need be considered.

Equating total thrust on the two sections as shown in figure 22.

$$\frac{f_m \; T \; B}{2 \quad 2} = f_{min} \; T \; B$$

Therefore, $f_{min} = \frac{f_m}{4}$

Thus the average strain causing deflection along the arch line is: -

$$\left(\frac{2 \; f_m}{3} + \frac{1 \; f_m}{4} \right) \frac{1}{2} = \frac{11}{24} \; f_m$$

Approximate length of the arch line is:-

$$= L + \frac{8 \; G^2}{3L}$$

The mean strain is $\frac{11 f_m}{24 \; E}$, where E is the modulus of elasticity. The total strain x becomes:-

$$x = \left(L + \frac{8G^2}{3L} \right) \; \frac{11}{24} \; \frac{f_m}{E}$$

Therefore the new arch height becomes:-

$G_1 = \frac{3L}{8} (\ell_1 - G)$ where ℓ_1 is the new arch length, ℓ - x. The process of calculating the new arch height may be repeated if necessary and by eqyatung the bending moment to the moment of resistance, as before, the stability.

of the beam can be determined.

VITA

Christopher Haycocks, the son of George F. and Louise K. Haycocks was born at Floriana, Malta, on the 27th of January, 1939.

He completed his primary and secondary education by receiving the Cambridge Overseas Higher School Certificate at St. Georges School, Kongwa, Tanganyika.

From Tanganyika he proceeded to England where he enrolled at the School of Metalliferous Mining, Camborne, Cornwall, in September 1958, and graduated in June of 1961 with the degree of Associateship of the Camborne School of Mines.

In September 1961 he enrolled at the Missouri School of Mines and Metallurgy to undertake studies toward the degree of Master of Science in Mining Engineering.